

Leakage radiation spectroscopy of organic/dielectric/metal systems: influence of SiO₂ on exciton-surface plasmon polariton interaction

J. Fiutowski^{*a}, T. Kawalec^{*b}, O. Kostiučenko^a, V. Bordo^a, H.-G. Rubahn^a, and L. Jozefowski^b
^aNanoSyd, Mads Clausen Institute, Syddansk Universitet, Alsion 2, DK-6400 Sønderborg, Denmark; ^bMarian Smoluchowski Institute of Physics, Jagiellonian University, Reymonta 4, 30-059 Krakow, Poland

ABSTRACT

Leakage radiation spectroscopy of organic para-Hexaphenylene (p-6P) molecules has been performed in the spectral range 420-675 nm which overlaps with the p-6P photoluminescence band. The p-6P was deposited on 40 nm silver (Ag) films on BK7 glass, covered with SiO₂ layers. The SiO₂ layer thickness was varied in the range 5-30 nm. Domains of mutually parallelly oriented organic nanofibers were initially grown under high-vacuum conditions by molecular beam epitaxy onto a cleaved muscovite mica substrate and afterwards transferred onto the sample by a soft transfer technique. The sample placed on a flat side of a hemisphere fused silica prism with an index matching liquid was illuminated under normal incidence by a He-Cd 325 nm laser. Two orthogonal linear polarizations were used both parallel and perpendicular to the detection plane. Spectrally resolved leakage radiation was observed on the opposite side of the Ag film (i.e. at the hemisphere prism) as a function of the scattering angle. Each spectrum contains a distinct peak at a wavelength dependent angle above the critical angle. This way the dispersion curve was measured, originating from a hybrid mode, i.e. the interaction between the p-6P excitons and surface plasmon polaritons (SPPs) of the metal/dielectric boundary. The presence of the SiO₂ layer considerably changes the dispersion curve in comparison to the one of the Ag/p-6P/air system. However, the Ag/SiO₂/p-6P/air stack forms a stable structure allowing construction of organic plasmonic devices such as nano-lasers.

Keywords: leakage radiation spectroscopy, exciton-plasmon coupling, p-6P nanofibers and films

1. INTRODUCTION

The field of plasmonics, which has been established and expanded during the last decade, comprises many physical phenomena, providing opportunities for controlling light-matter interaction on the nanoscale [1-4]. One of the main routes in the field was focused on photonic nanowires and nanofibers, which as hybrid structures were able to combine both plasmonic and photonic components. Such an assembly suggests new challenges in the design and application of nanophotonic circuits by integrating active surface plasmon based elements, which can convert optical signals to plasmonic signals and vice versa [4].

Several systems based on organic nanofibers have been already proposed and successfully exploited, where organic nanofibers were used both as passive and active local surface plasmon polariton (SPP) sources [8, 9] as well as passive dielectric-loaded SPP waveguides [10-12].

Unique optical properties of these materials, both tailorable linear and nonlinear as well as optoelectronic properties [13-15], prove a great potential for further development in the field of active nanoplasmonics.

The most common SPP excitation techniques are the Kretschmann configuration, where a laser beam undergoes total internal reflection at a prism surface covered with a thin metallic film (usually gold or silver), and metallic grating couplers, where optimized momentum matching is achieved by an appropriate grating constant. The alternative hybrid system described here allows for direct excitation of SPPs on a flat silver surface upon direct UV illumination of submicron sized molecular emitters located close to the metal surface.

*fiutowski@mci.sdu.dk; tomasz.kawalec@uj.edu.pl

We report the study of a hybrid system represented by organic (para-Hexaphenylene, *p*-6P), mutually parallelly oriented nanofibers, separated from a thin silver surface by a SiO₂ layer with a thickness in the range of 5 to 30 nm. To demonstrate SPP generation, we have successfully exploited a reversed Kretschmann configuration, where SPPs excited on the metal-dielectric interface leak energy through the metal film into glass at angles higher than the critical one [16-18].

Performing these measurements as a function of wavelength allows one to derive dispersion relations for SPPs.

2. EXPERIMENTAL

2.1 Sample fabrication

The samples consist of 500 μm BK7 glass, both-side polished plates, coated on one side with a 40 nm silver layer. Metal films, evaporated by an e-beam deposition technique, were in the next step RF-sputtered with a thin SiO₂ layer in the range of 5 to 30 nm and covered with *p*-6P nanofibers on top. In order to perform the latter step, domains of mutually parallel oriented organic nanofibers were grown under high-vacuum conditions by molecular beam epitaxy of *p*-6P molecules onto a freshly cleaved muscovite mica surface [19]. In order to achieve the appropriate molecules' mobility at the surface, the mica sheet was placed between two heated plates ensuring a surface temperature of around 430 K. The evaporation was done using a custom-built Knudsen cell made from a 40 mm long stainless steel container with a coaxial cable as heating element. Typical lengths of nanofibers ranged to several hundred micrometers, widths of the order of 400 nm, and heights between a few tens and one hundred nanometers. Afterwards, fibers were transferred from the growth to the sample surface using a recently developed soft and large scale rolling transfer technique [20].

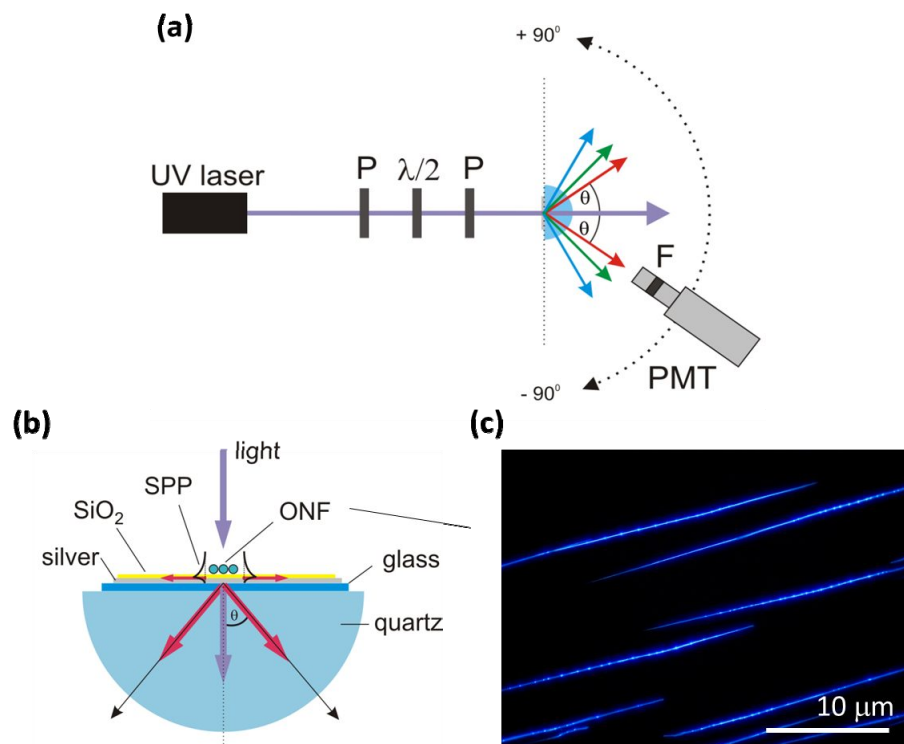


Figure 1. (a) Experimental setup; P - polarizer, $\lambda/2$ - half-wave plate, F - filter, PMT - photomultiplier. (b) Zoom on the half-sphere with the sample mounted on the flat side; ONF - organic nanofiber. (c) Epifluorescence microscopy image of *p*-6P nanofibers upon UV excitation.

2.2 Experimental setup

Each sample was placed on the flat surface of a 10 mm radius quartz hemisphere with the help of an immersion oil ($n = 1.5000 \pm 0.0001$) – see Fig. 1. The excitation of *p*-6P nanofibers was performed by a He-Cd 325 nm laser, where two orthogonal linear polarizations were considered (TE and TM). The polarizations were controlled with a polarizer and a half-wave plate. The chosen domain of nanofibers of a millimeter size was precisely positioned in the center of the hemisphere and in the center of rotation of the set-up. To fulfill the conditions of leakage radiation spectroscopy the excitation light was directed normal to the sample plane (0 degrees) and the scattered light was detected on the other side of the hemisphere by a photo multiplier tube (PMT) mounted on a motorized rotating arm, with an angular resolution of 0.1 degrees, in steps of 0.5 degrees, in the range from $\Theta = -90$ to $+90$ degrees. In the case of UV excitation the detection spectral range was 420-675 nm, overlapping with the *p*-6P photoluminescence band [21]. Spectral definition was ensured by a set of narrow band-pass interference filters mounted in front of the PMT.

First the samples were examined in an epifluorescence microscope to find the best quality domains of nanofibers and to find the direction of their long axes. Precise positioning of the sample on the half-sphere ensured that the best domain of nanofibers of a desired direction of fibers (perpendicularly to the observation plane) was centered. Then a fine adjustment of the half-sphere was performed to set the illuminated domain of the sample in the center of rotation of the set-up. Finally the scan was run from -90 till $+90$ degrees.

3. RESULTS AND DISCUSSION

A typical scan performed for a sample consisting of 40 nm of Ag, 20 nm of SiO₂ and *p*-6P nanofibers on top is shown in Fig. 2. Two symmetrically positioned maxima of transmitted light above the critical angle are observed as leakage radiation signal. The central maximum stems from laser light passing directly through the sample. The small maxima are formed by light scattered off the interference filter edges. To calculate the leakage signal angle for each wavelength the arithmetic mean of both maxima positions were taken. This way possible systematic errors caused by a imperfect set-up geometry are reduced.

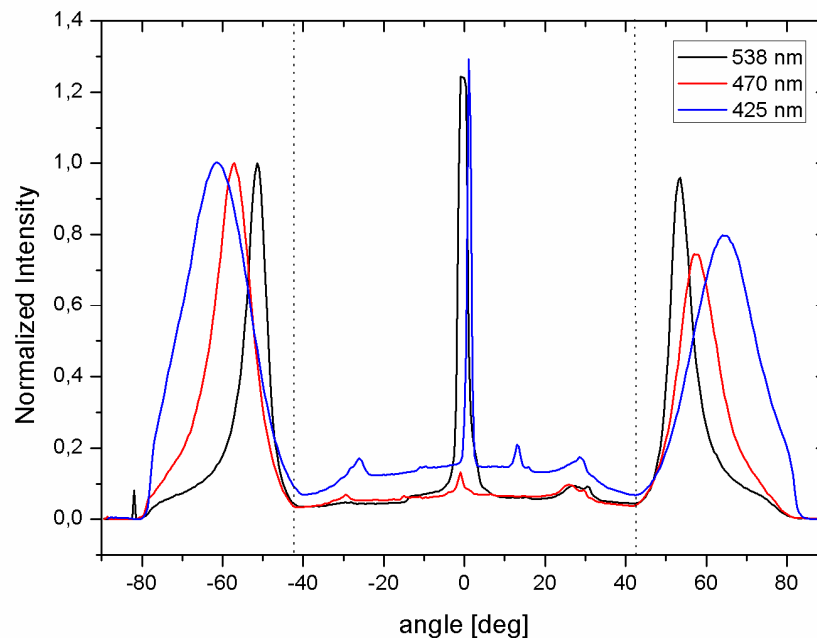


Figure 2. Leakage radiation as a function of Θ . Excitation wavelength was 325 nm, and detection was at 425, 470 and 538 nm, respectively. Vertical dotted lines indicate positions of the critical angle.

The leakage radiation angles Θ versus wavelength are plotted in Fig. 3 a)-e) as red circles for various thicknesses of the SiO₂ layers (0, 5, 12, 20, 30 nm). To model the hybrid system, an analytical approach was used. Due to the boundary conditions for electric and magnetic fields at interfaces, the wave vector component parallel to the sample surface is the same in all layers. This implies that the angle which corresponds to a peak in the leakage radiation spectrum coincides with the incidence angle at which a dip in the attenuated total reflection (ATR) spectrum is observed. Thus, the angles at which plasmonic modes are excited were computed for the ATR of a plane electromagnetic wave in the Kretschmann configuration instead of the experimentally employed anti-Kretschmann one. The calculations were based on a matrix formulation of Fresnel equations for an arbitrary number of dielectric as well as metallic layers [22]. The ATR spectra were found for an infinite layer of fused silica, 0.5 mm of glass, and the experimentally implemented thickness of SiO₂ and *p*-6P layers. The indices of refraction for fused silica, glass, silver and SiO₂ are widely accessible and the complex index of refraction for *p*-6P is taken from [23].

To estimate the role of the *p*-6P nanofiber emitters on the SPPs dispersion relation, calculations were performed for a range of effective *p*-6P layer thicknesses. The best agreement between experimental and analytical results was found for the case where the organic layer was not taken into account in the calculations. Results obtained in this regime are shown in Fig. 3 a)-e) as black squares. A small discrepancy between experiment and calculations seen for the first two cases in Fig. 3 (0 nm and 5 nm of SiO₂ layer) is presumably due to a strong coupling between molecular excitons and SPPs modes, which is not considered in the theoretical model.

The calculations for various thicknesses of the SiO₂ layer are summarized in Fig. 3 f). The results for 20 and 50 nm of the effective thickness of the *p*-6P layer definitely do not fit the experimental points shown in b). Thus, the SPPs dispersion relation is governed mainly by the properties of the silver-SiO₂ interface.

4. CONCLUSIONS

In the present paper we have shown measurements of angular spectra of leakage radiation registered from a hybrid nanostructure represented by *p*-6P organic nanofibers separated from a metallic film by a dielectric gap. We have identified peaks in the angular leakage spectra which originate from SPP excitation and have plotted the dispersion relation for a dielectric gap layer thickness in the range 0-30 nm. The dispersion curves indicate the existence of N effective channel of energy transfer between organic nanofibers and the substrate structure. In such a case the *p*-6P nanofibers plays the role of a local source of SPP excitation.

5. ACKNOWLEDGMENTS

Financial funding of this work was provided by the Polish "National Science Centre" grant N N202 013940 as well as by the Danish Council for Independent Research (FTP-project No. 09-072949 ANAP).

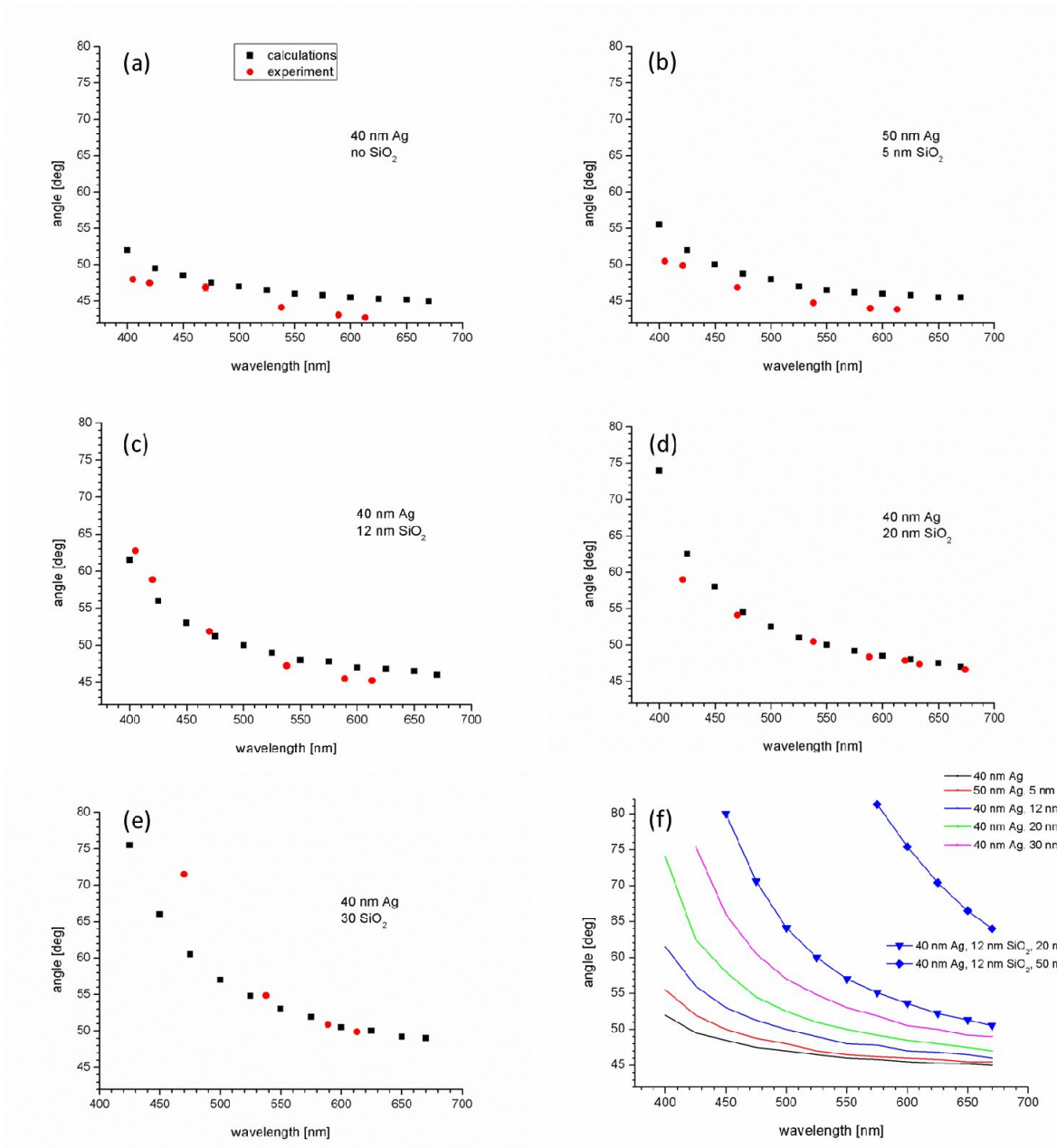


Figure 3. Angular dispersion curves, both calculated and measured for various layer configurations. (a) to (e) are measurements (red dots) and calculations (black squares) for various thicknesses of SiO₂. (f) summarizes the calculations (solid lines) and includes also calculations using two different p6P thicknesses (lines with symbols).

REFERENCES

- [1] Maier S. A., [Plasmonics: Fundamentals and Applications], Springer, (2007).
- [2] Lal S., Link S., and Halas N. J., "Nano-optics from sensing to waveguiding," *Nat. Photonics* 1, 641–648 (2007).
- [3] Anker J. N., Hall W. P., Lyandres O., Shah N. C., Zhao J., and Van Duyne R. P., "Biosensing with plasmonic nanosensors," *Nat. Mater.* 7, 442–453 (2008).

- [4] Ebbesen T. W., Genet C., and Bozhevolnyi S. I., "Surface-plasmon circuitry," *Phys. Today* 61(5), 44–50 (2008).
- [5] Radko I. P., Bozhevolnyi S. I., Brucoli G., Martín-Moreno L., García-Vidal F. J., and Boltasseva A., "Efficiency of local surface plasmon polariton excitation on ridges," *Phys. Rev. B* 78(11), 115115 (2008).
- [6] López-Tejiera F., Rodrigo S. G., Martín-Moreno L., García-Vidal F. J., Devaux E., Ebbesen T. W., Krenn J. R., Radko I. R., Bozhevolnyi S. I., González M. U., Weeber J. C., and Dereux A., "Efficient unidirectional nanoslit couplers for surface plasmons," *Nat. Phys.* 3(5), 324–328 (2007).
- [7] Bharadwaj P., Bouhelier A., and Novotny L., "Electrical excitation of surface plasmons," *Phys. Rev. Lett.* 106(22), 226802 (2011).
- [8] Skovsen E., Søndergaard T., Fiutowski J., Rubahn H.-G. and Pedersen K., "Surface plasmon polariton generation by light scattering off aligned organic nanofibers," *J. Opt. Soc. Am. B* 29(2), 249 (2012).
- [9] Skovsen E., Søndergaard T., Fiutowski J., Simesen P., Osadnik A., Lützen A., Rubahn H.-G., Bozhevolnyi S. I. and Pedersen K., "Local excitation of surface plasmon polaritons by second-harmonic generation in crystalline organic nanofibers," *Opt. Express* 20(15), 16715–16725 (2012).
- [10] Radko I. P., Fiutowski J., Tavares L., Rubahn H.-G., and Bozhevolnyi S. I., "Organic nanofiber-loaded surface plasmon-polariton waveguides," *Opt. Express* 19, 15155–15161 (2011).
- [11] Leißner T., Lemke C., Fiutowski J., Radke J. W., Klick A., Tavares L., Kjelstrup-Hansen J., Rubahn H.-G. and Bauer M., "Morphological tuning of the plasmon dispersion in dielectric-loaded nanofiber waveguides," *Phys. Rev. Lett.* 111, 046802 (2013).
- [12] Leißner T., Lemke C., Jauernik S., Müller M., Fiutowski J., Kjelstrup-Hansen J., Magnussen O., Rubahn H.-G., and Bauer M., "Surface plasmon polariton propagation in organic nanofiber based plasmonic waveguides," *Opt. Express* 21(7), 8251 (2013).
- [13] Brewer J., Schiek M., and Rubahn H.-G., "Nonlinear optical properties of CNHP4 nanofibers: Molecular dipole orientations and two photon absorption cross-sections," *Opt. Comm.* 283(7), 1514–1518 (2010).
- [14] Pedersen K., Schiek M., Rafaelsen J., and Rubahn H.-G., "Second-harmonic generation spectroscopy on organic nanofibers," *Appl. Phys. B* 96(4), 821–826 (2009).
- [15] Kjelstrup-Hansen J., Simbrunner C., and Rubahn H.-G., "Organic surface-grown nanowires for functional devices," *Rep. Prog. Phys.* 76, 126502/1-24 (2013).
- [16] Gryczynski I., Malicka J., Gryczynski Z., and Lakowicz J. R., "Surface plasmon-coupled emission with gold films," *J. Phys. Chem. B* 108, 12568–12574 (2004).
- [17] Trnavsky M., Enderlein J., Ruckstuhl T., McDonagh C., and MacCraith B. D., "Experimental and theoretical evaluation of surface plasmon-coupled emission for sensitive fluorescence detection," *J. Biomed. Opt.* 13, 054021 (2008).
- [18] Chowdhury M. H., Ray K., Geddes C. D., and Lakowicz J. R., "Use of silver nanoparticles to enhance surface plasmon coupled emission (SPCE)," *Chem. Phys. Lett.* 452, 162–167 (2008).
- [19] Kankate L, Balzer F, Niehus H, and Rubahn H.-G., "From clusters to fibers: parameters for discontinuous p-6P thin film growth," *J. Chem. Phys.* 128, 084709 (2008).
- [20] Tavares L., Kjelstrup-Hansen J. and Rubahn H.-G., "Efficient roll-on transfer technique for well-aligned organic nanofibers," *Small* 7, 2460–3 (2011).
- [21] Balzer F. and Rubahn H. R., "Dipole-assisted self-assembly of light-emitting p-nP needles on mica," *Appl. Phys. Lett.* 79, 3860–3860 (2001).
- [22] Sernelius B. E., [Surface Modes in Physics], Wiley-VCH (2001).
- [23] Kostiučenko O., Fiutowski J., Kawalec T., Bordo V., Rubahn H.-G., and Jozefowski L., "Surface plasmon polariton dispersion relation at silver/dielectric interfaces," *Opt. Comm.* – in preparation